Journal of Mathematical Chemistry Vol. 38, No. 4, November 2005 (© 2005)
DOI: 10.1007/s10910-004-6894-7

From the cube to the Dyck and Klein tessellations: Implications for the structures of zeolite-like carbon and boron nitride allotropes

R. Bruce King *
Department of Chemistry, University of Georgia, Athens, Georgia 30606, USA
E-mail: rbking@sunchem.chem.uga.edu

Mircea V. Diudea
Faculty of Chemistry and Chemical Engineering, Babeş-Bolyai University, Cluj-Napoca, Roumania

Received 4 November 2004; revised 14 December 2004

Geometrical transformations can be described which have the effect of multiplying the numbers of vertices in a trivalent polyhedron by three, four, or seven. Tripling the cube by the so-called leapfrog transformation gives the truncated octahedron. Quadrupling the cube followed by identifying the square faces to give a genus 3 surface gives the Dyck surface of 12 octagons. Septupling the cube by the so-called capra transformation followed by identifying the square faces to give a genus 3 surface gives the Klein surface of 24 heptagons. These geometrical transformations relate to the construction of low-density zeolite-like structures for carbon and boron nitride allotropes based on a cubic lattice.

KEY WORDS: Dyck tessellation, Klein tessellation, Carbon, boron nitride

AMS subject classification: 52B10, 92E10

1. Introduction

The experimentally known carbon allotropes are of four types, namely diamond, graphite, fullerenes, and nanotubes. Diamond and graphite have been known since antiquity whereas fullerenes were first isolated in the late 1980s and nanotubes a few years later. The structure of diamond consists of an isotropic infinite network of tetrahedrally hybridized carbon atoms in all directions whereas the structures of the other carbon allotropes are based on trigonal carbon atoms. The structure of graphite consists of a flat sheet of carbon hexagons whereas the fullerenes [1] are closed polyhedra generally having 12 pentagonal faces and various

*Corresponding author.

0259-9791/05/1100-0425/0 © 2005 Springer Science+Business Media, Inc.

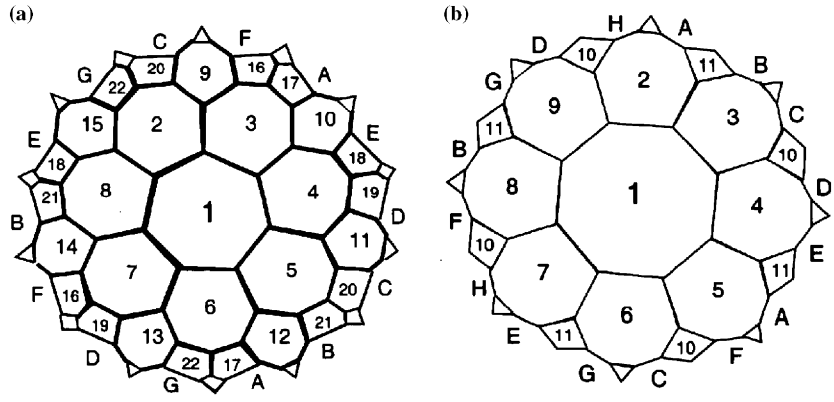

Figure 1. (a) The Klein tessellation {7,3}. (b) The Dyck tessellation {8,3}; In both, cases the edges with identical letters (A→H or G) are identified to embed the tessellation in a genus 3 surface.

numbers of hexagonal faces. The first such fullerene to be isolated was the truncated icosahedral C_{60}. In the carbon nanotubes a network of carbon hexagons similar to the planar sheets in graphite is folded over and joined to form a tube using positively curved pentagonal faces to close the ends of the tube.

Carbon structures based on networks of trigonal carbon atoms having only hexagonal and larger faces, e.g., heptagons and/or octagons, have been proposed in the literature during the last 15 years. The presence of faces larger than hexagons leads to sites of negative curvature and precludes the formation of closed polyhedra when there are no compensating pentagonal, quadrilateral, or triangular faces of positive curvature. The trivial name schwarzite has been suggested for these still unknown carbon allotropes in honor of the mathematician H.A. Schwarz, who first studied the relevant negative curvature surfaces in detail [2].

The theoretical possibility of negative curvature allotropes of carbon was apparently first recognized by Mackay and Terrones [3], who proposed the P192 schwarzite structure with a unit cell of 192 carbon atoms consisting of hexagons and octagons in a simple infinite cubic lattice. Their proposed structure was quickly followed by the 216 atom unit cell P216 and D216 schwarzite structures of Lenosky, Gonze, Teter, and Elser [4], consisting of hexagons and heptagons in a similar cubic lattice. A structure with only hexagons and heptagons in a cubic lattice with a smaller unit cell was the D168 schwarzite structure of Vanderbilt and Tersoff [5]. In 1996 King [6] first showed the connection between the D168 schwarzite structure of Vanderbilt and Tersoff and the classical Klein tessellation [7] (figure 1(a)) consisting of 24 regular heptagons embedded in a genus 3 surfaces. The leapfrog transformation [8] used to triple the regular dodecahedron into the truncated icosahedron of C_{60} (figure 2(a)) can also be used to triple the Klein tessellation (figure 1(a)) into the D168 schwarzite structure. In both cases

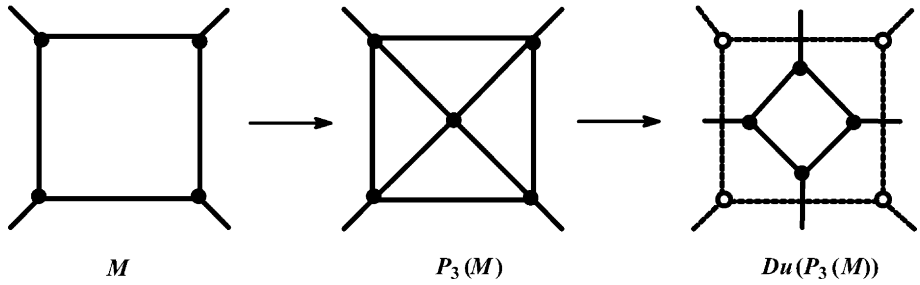

Figure 2. Leapfrogging a squared face of a trivalent map.

the leapfrog transformation introduces the minimum number of hexagons so that no pair of non-hexagons shares an edge. In the case of fullerenes this leads to the so-called "isolated pentagon rule."

The Klein tessellation is named after the 19th century German mathematician Felix Klein. One of his students, Walther Dyck, discovered a genus 3 tessellation of 12 regular octagons (figure 1(b)) [9]. A leapfrog transformation on the Dyck tessellation leads to a structure consisting of a 96-vertex unit containing only hexagons and octagons. This is a potential unit cell not only for possible carbon allotropes but also boron nitride $(BN)_x$ allotropes. In this connection the most thermodynamically stable boron nitride allotropes have only heteronuclear BN bonds, which is only possible if all of the faces have an even number of edges, e.g., squares, hexagons, or octagons.

The Klein and Dyck tessellations (figure 1) are networks of polygons embedded on a genus 3 surface, i.e., a sphere with three handles. The significance of genus 3 is that such a surface can be isotropic in all three directions unlike genus 1 and 2 surfaces, which must necessarily be anisotropic. The sphere with three handles is topologically homeomorphic to a cube with three tubes connecting pairs of faces in an isotropic manner. If the three tubes all connect adjacent (*cis*) faces of the cube similar to the bidentate ligands in a tris(bidentate) octahedral metal complex, then the resulting genus 3 surface can be a finite structure similar to the tessellations discussed by Klein and Dyck in their 19th century papers (figure 1). However, the relevant alternative is a chain of *trans* connections of opposite faces of the cubic unit cells leading through infinity to a cubic lattice with a zeolite-like structure.

The unit cell in these zeolite-like structures proposed for these carbon and boron nitride allotropes is a cube with congruent holes in each of its six faces known as a plumber's nightmare (see below). This paper describes transformations that lead directly from the original cube to the Dyck and Klein tessellations (figure 1) embedded on the surface of the cube. Such transformations demonstrate the relationship of these genus 3 tessellations to a cubic lattice.

2. Tripling the cube to the truncated octahedron: The leapfrog transformation

The leapfrog Le (tripling) transformation [8,10,11] (figure 2) consists of P_3 capping (*i.e.*, polygonal 3-capping, stellating) each face followed by dualization thereby generating a network of $3n$ vertices from any network of n vertices (each having degree 3). In the above, the omnicapped P_3 network forms a pair with its dual, which interchange by dualization.

The leapfrog operation can be written as follows [11]:

$$\mathrm{Le}(M) = \mathrm{Du}(P_3(M)) = \mathrm{Tr}(\mathrm{Du}(M)) \tag{1}$$

A sequence of stellation-dualization rotates the parent s-gonal faces by π/s. The P_s ($s = 3, 4, 5$) symbol denotes a capping, by polygons of size s, operation [11].

Applying this process to the cube C gives the truncated octahedron (figure 3), which has $3 \times 8 = 24$ vertices, 36 edges, and 14 faces. This is a reasonable polyhedron for a molecular allotrope of boron nitride, $B_{12}N_{12}$, since the boron and nitrogen atoms can be located at alternate vertices so that all 36 edges correspond to B–N bonds with no direct B–B or N–N bonds, which are less energetically favorable [12–14].

It is possible to carry the leapfrog transformation of the cube even beyond the truncated octahedron to give a genus 3 tessellation that could be the building block of an infinite cubic lattice based on the plumber's nightmare (figure 4(a)). In this connection the surface is removed at each of the six square faces of the truncated octahedron to generate square holes in the six faces of a plumber's nightmare with one hexagon in each octant. Identifying pairwise the square holes of adjacent such units provides the three handles of a genus 3 surface having $24/2 = 12$ vertices (of degree 4), $(24/2) + 12 = 24$ edges, and 8 faces (hexagons) per unit (figure 3(b)), consistent with Euler's theorem, namely $v - e + f = 2 - 2g$ where v, e, f, and g are the numbers of vertices, edges, and faces and the genus, respectively.

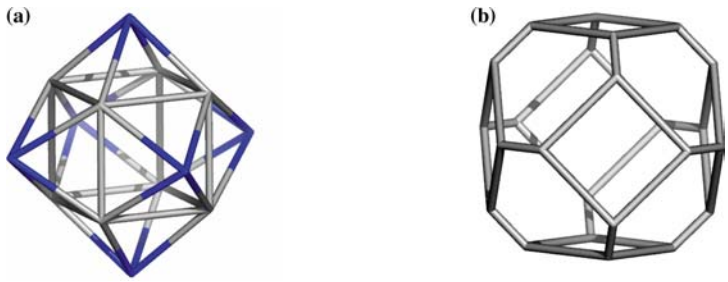

Figure 3. P_3 omnicapping of the cube C (a); Dual of P_3 (C), *i.e.*, the Le(C) transform. The two objects form a pair with its dual, which interchange by dualization.

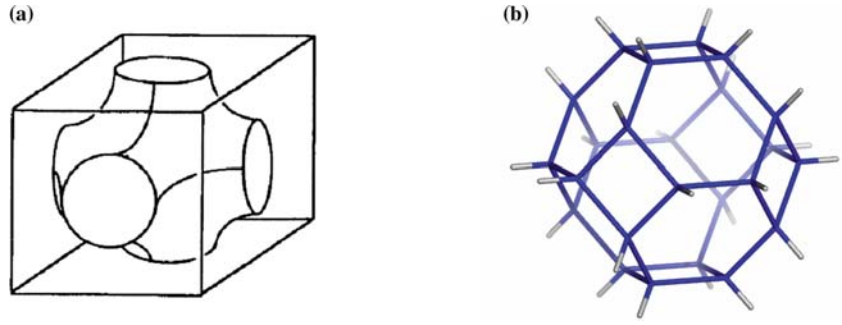

Figure 4. Two descriptions of the unit cell of a P surface: (a) The "plumber's nightmare" octahedral junction of six pipes through the faces of a cube; (b) An infinite lattice (of degree 4) embedded in a genus 3 surface, with a repeat unit derived from Le(C).

This structure is one of the Platonic tessellations [15,16] of genus 3 and is the dual of the tessellation corresponding to the double cube group [17,18], designated as ${}^2W_h$. In addition, an infinite cubic lattice can be built from this genus 3 building block if the square holes are identified with the square hole in an adjacent equivalent genus 3 unit and this process is extended to infinity in all three directions.

The necessarily negatively curved octants in this plumber's nightmare (figure 4(a)) structure create too much strain in the hexagonal faces for this to be an energetically favorable structure in an actual carbon or boron nitride allotrope. This is true whether the allotrope in question is either molecular consisting of a single genus 3 unit with identified square holes or polymeric consisting of an infinite cubic lattice of these building blocks joined as discussed above. This structure thus has no heptagonal or octagonal faces to provide a natural site for this required negative curvature. Nevertheless, this construction is a useful model for understanding related procedures for converting a cube to the Dyck and Klein tessellations (figure 1) that are of greater possible chemical interest.

3. Quadrupling the cube to the Dyck tessellation: The chamfering transformation

The quadrupling transformation [19–21] (figure 5) is another composite operation, achieved by the sequence:

$$Q(M) = E_-(\mathrm{Tr}_{P_3}(P_3(M))) \tag{2}$$

where E_- means the (old) edge deletion (dashed lines, in figure 5) of the truncation Tr_{P3} of each vertex where P_3 capping faces of a parent face are incident. Note that the orientation of parent faces is preserved.

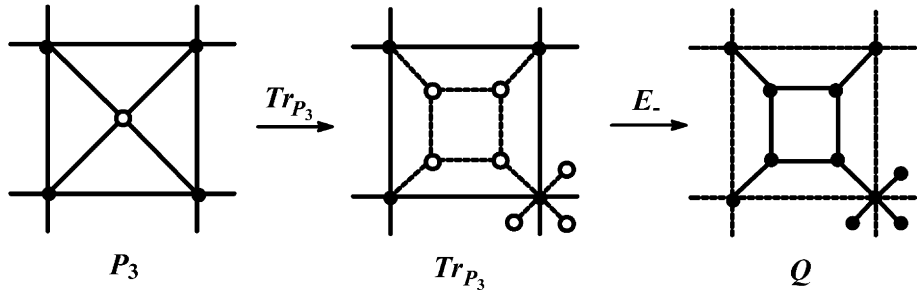

Figure 5. Quadrupling a square face of a 4-valent map.

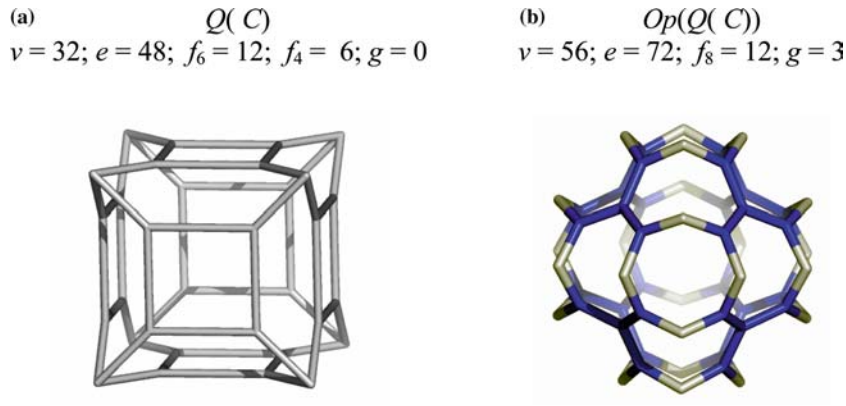

Figure 6. Quadrupling/chamfering the cube (a) and the unit of 32 atoms, representing the Dyck graph, within an infinite lattice, embedded in a genus 3 negatively curved surface (b).

The E_- edge deletion in the above operation sequence corresponds to the woodworking operation known as chamfering in which the edges of an object are planed to faces; hence this operation on polyhedra is also known as chamfering.

Quadrupling the cube generates a closed polyhedron with 6 square faces, 12 hexagonal faces, 48 edges and 32 vertices (figure 6(a)). The number of vertices of the cube is thus quadrupled from 8 to 32. This polyhedron obeys the "isolated square rule" in which no pair of square faces shares an edge. Strout [22] has shown by density functional methods that this structure for $B_{16}N_{16}$ constructed from squares and hexagons is much more stable than alternative structures constructed from pentagons and hexagons.

The above operation can continue with bisection of the edges bounding the parent-like faces (i.e., those resulting from Tr_3). This leads to "open faces" having alternating divalent and trivalent boundary vertices. The size of the hexagons surrounding the open faces enlarges by n, thus leading to sites of negative curvature. The last simple operation was called [11] Op_n. In the case of quadrupling, the sequence leading to open objects is written as follows:

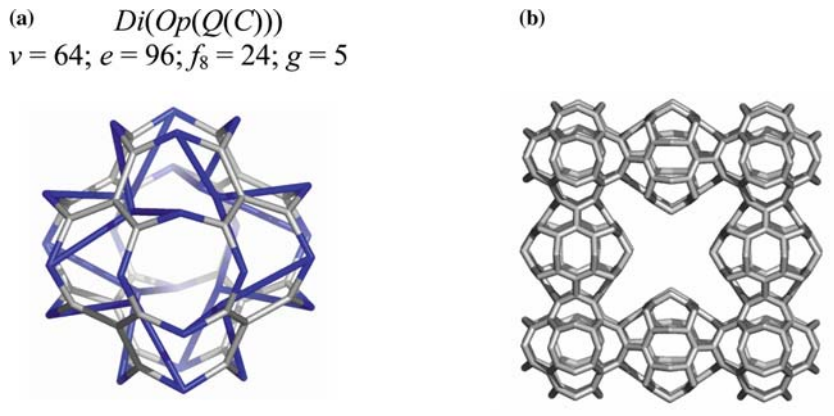

Figure 7. Trivalent finite (a) and infinite (b) representations of the Dyck tesselation, embedded in surfaces of genus g $\geqslant$ 3. Di, Op, Q denote dimerization, opening and quadrupling operations.

$$\mathrm{Op}_n(Q(M)) = \mathrm{Op}_n(\mathrm{Tr}_{P3}(P_3(M)) \tag{3}$$

and is exemplified in figure 6(b) as $\mathrm{Op}_n(Q(C))$ The open faces (i.e., holes) in this structure can participate in the construction of infinite lattices embedded on surfaces of negative curvature and genus $g = 3$. As a result of the Op_n operation, the π-electron networks of molecules associated with such graphs exhibit open-shell structures including non-bonding orbitals.

Returning to the object in figure 6(b), among the 18 octagons, 6 of them (those arising from the square faces by the Op_n operation) become the holes in a plumber's nightmare (figure 4(a)) and are identified pairwise to make a genus 3 surface. This can either be a finite genus 3 surface with three handles connecting adjacent holes or an infinite cubic lattice connecting the holes in adjacent similar plumber's nightmares [23]. The remaining 12 octagonal faces become the 12 octagonal faces of a Dyck tessellation (figure 1(b)) embedded on the genus $g \geqslant 3$ surface, whether finite (figure 7(a)) or infinite (figure 7(b)). The "dimerization" Di operation requires the pairwise identification of all the open faces of two units, e.g., those shown in figure 6(b). In other words, the vertices of the parent polyhedron (e.g., the cube) are connected to the degree 2 vertices lying in three neighboring open faces. The finite object thus obtained has only degree 3 vertices (figure 7(a)).

Note that in applying the Op_1 operation to $Q(C)$, the numbers of vertices and edges are apparently doubled by the edge bisection procedure (figure 6(b)). The resulting "dimer" (figure 7(a)) has just doubled parameters. These numbers are then halved to the original 32 vertices, 48 edges and 12 octagonal faces, when the six "open faces"/holes are identified. The same is true for an infinite lattice

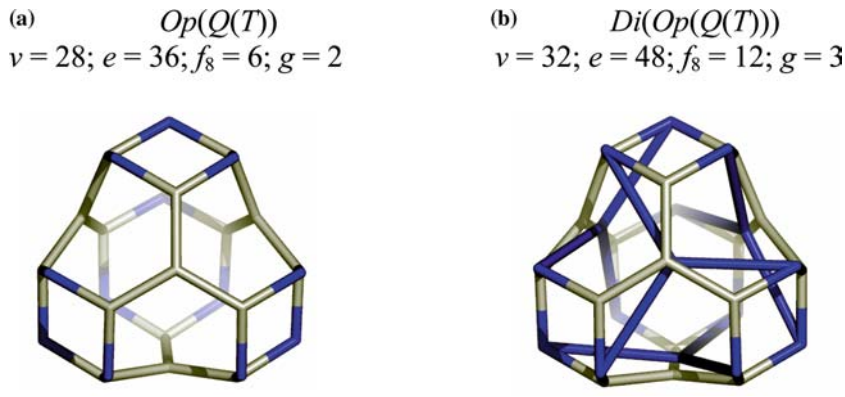

Figure 8. Precursors of the finite representation of the Dyck graph.

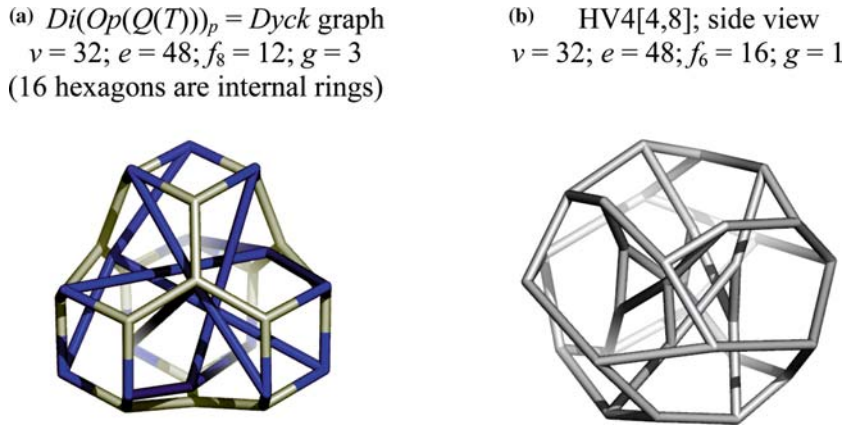

Figure 9. The graph of Dyck, embedded in a tetrahedral (a) and toroidal (b) surface.

derived from the unit in figure 6(b) (see figure 7(b)). However, the dimeric object having the Dyck tessellation is not the true finite, trivalent Dyck graph.

The above sequence of operations, applied on the tetrahedron (figure 8), enabled Diudea [11] to find the Dyck graph.

Among the 6^4 permutations on the dimer in figure 8(b), a trivalent finite graph having all the characteristics (number of cycles, eigenvalues, etc., identical to the literature data of the Dyck graph [24]) was found (figure 9(a)). By using the Torus software package, Diudea [11] succeeded in drawing the 3D toroidal representation (figure 9(b)), first predicted by Ceulemans et al. [25].

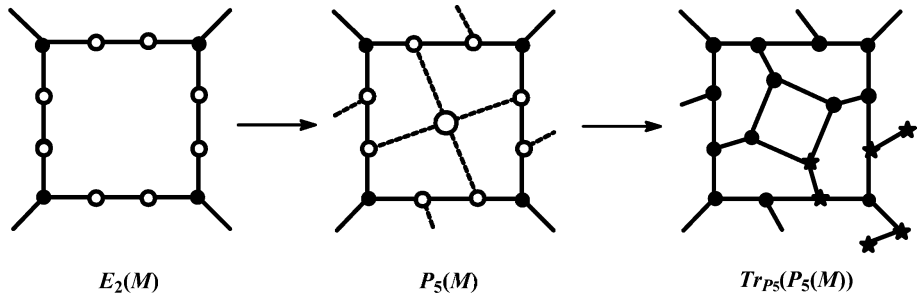

Figure 10. Septupling a square face of a 3-valent map.

4. Septupling the cube to the Klein tessellation: The capra transformation

The septupling transformation [11,26], called the capra transformation (*capra* = goat in Roumanian) by analogy with the designation of the tripling transformation as the leapfrog transformation, is achieved by truncating the vertex located in the center of parent faces of a pentangulation P_5 transform (figure 10). Note that, P_5 involves an E_2 (i.e., edge trisection). This operation results in a map that preserves the original vertices while the parent s-gonal faces are twisted by $\frac{1}{4}/(\frac{3}{2})s$.

The transformation can be written [26] as follows:

$$\mathrm{Ca}(M) = \mathrm{Tr}_{P5}(P_5(M)) \tag{4}$$

with Tr_{P5} meaning the truncation of each vertex where P_5 capping faces of a parent face are incident.

The septupling transformation insulates any face of M by its own hexagons, which are not shared with any of the other original faces (in contrast to *Le* or Q – see figure 11(a)). This operation is clearly related to $Q(M)$ (compare equations (2) and (4)). The multiplication ratio is $2d + 1$, which gives 7 in case of a cubic cage (i.e., having all vertices of degree d=3) [26].

The Ca operation can continue by an E_n homeomorphic transformation of the edges bounding the parent-like faces (i.e., those resulted by Tr_5) thereby leading to open maps with all polygons of the same (6+n) size. The sequence leading to open objects within this operation can be written as follows:

$$\mathrm{Op}_n(\mathrm{Ca}(M)) = \mathrm{Op}_n(\mathrm{Tr}_{P5}(P_5(M))) \tag{5}$$

The Op_1 objects (i.e., molecules) have open-shell π-electronic structures leading to non-bonding orbitals.

Applying the septupling transformation to the cube gives the objects in figure 11. Note that all faces in Op(Ca(C)) (figure 11(b)) are heptagons while the open faces are twice the size of the parent faces (i.e., octagons).

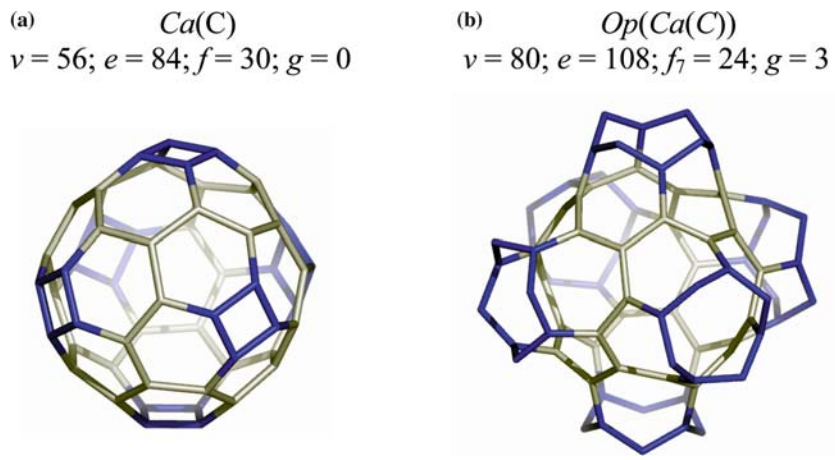

Figure 11. Capra transforms of the cube, as finite cage (a) and the unit of an infinite lattice.

The vertices in figure 11(b) relative to the faces of the original cube can be classified into the following three types:

(1) The eight original vertices of the cube, which are each shared by three faces.

(2) The $2 \times 12 = 24$ new vertices obtained by an E_2 operation on the original cube. Each of these vertices is shared by two faces of the original cube.

(3) The $8 \times 6 = 48$ vertices of the six open, octagonal faces. Each of these vertices is unique to a single face. However, these vertices are identified pairwise to give $48/2 = 24$ vertices in the final figure.

Adding up the total number of vertices of the three types gives $8 + 24 + 24 = 56$ total vertices. Similarly the edges in figure 11(b) are of the following three types:

(1) The 36 new edges obtained by trisecting the 12 edges of the original cube. Each of these edges is shared by two faces of the original cube.

(2) The $4 \times 6 = 24$ edges connecting the octagonal face to vertices of the original cube. Each of these edges is unique to a single face.

(3) The $8 \times 6 = 48$ edges of the six octagonal faces. Each of these vertices is unique to a single face. However, these vertices are identified pairwise to give $48/2 = 24$ edges in the final figure.

Adding up the total number of edges of the three types gives $36+24+24 = 84$ total edges. The resulting genus 3 figure with 24 heptagonal faces, 56 vertices, and 84 edges is the Klein tessellation (figure 1(a)).

5. Summary

This paper shows how the cube can be related to the truncated octahedron, the Dyck tessellation, and the Klein tessellation by the tripling (leapfrog), quadrupling (chamfering), and septupling (capra) transformations, respectively. The last two relationships are useful for constructing possible cubic structures for low-density zeolite-like carbon and boron nitride allotropes containing seven- and eight-member rings as well as six-membered rings.

Acknowledgment

One of us (RBK) is indebted to the National Science Foundations for partial support of this work under Grant CHE-0209857.

References

[1] H.W. Kroto, A.W. Allaf and S.P. Balm, Chem. Rev. 91 (1991) 1212.
[2] H.A. Schwarz, *Gesammelte Mathematische Abhandlungen* (Springer, Berlin, 1890).
[3] A.L. Mackay and H. Terrones, Nature 352 (1991) 762.
[4] T. Lenosky, X. Gonze, M. Teter and V. Elser, Nature 355 (1992) 333.
[5] D. Vanderbilt and J. Tersoff, Phys. Rev. Lett. 68 (1992) 511.
[6] R. B. King, J. Phys. Chem. 100 (1996) 15096.
[7] F. Klein, Math. Ann. 14 (1879) 428; F. Klein, *Gesammelten Mathematischen Abhandlungen* (Springer-Verlag, Berlin, 1923), Vol. 3, pp. 90–136.
[8] P.W. Fowler and D.B. Redmond, Theor. Chim. Acta 83 (1992) 367.
[9] W. Dyck, Math. Ann. 17 (1880) 510.
[10] M.V. Diudea, P.E. John, A. Graovac, M. Primorac and T. Pisanski, Croat. Chem. Acta 76 (2003) 153.
[11] M.V. Diudea, Forma 19 (2004) 131.
[12] I. Silaghi-Dumitrescu, F. Lara-Ochoa and I. Haiduc, J. Mol. Struct. (Theochem) 370 (1996) 17.
[13] G. Seifert, P.W. Fowler, D. Mitchell, D. Porezag and T. Frauenheim, Chem. Phys. Lett. 268 (1997) 352.
[14] H.-S. Wu, X.-H. Xu, F.-Q. Zhang and H. Jiao, J. Phys. Chem. A, 107 (2003) 6609.
[15] D. Singerman and P.D. Watson, Geom. Ded. 66 (1997) 69.
[16] R.B. King, J. Mol. Struct. 656 (2003) 119.
[17] R.B. King, Mol. Phys. 100 (2002) 297.
[18] R.B. King, Mol. Phys. 102 (2004) 1231.
[19] P.W. Fowler, J.E. Cremona, and J.I. Steer, Theor. Chim. Acta 73 (1988) 1.
[20] A. Deza, M. Deza, and V. P. Grishukin, Discrete Math. 192 (1998) 41.
[21] A. Ceulemans, R.B. King, S.A. Bovin, K.M. Rogers, A. Troisi and P.W. Fowler, J. Math. Chem. 26 (1999) 101.
[22] D.L. Strout, Chem. Phys. Lett. 383 (2004) 95.
[23] Cs. L. Nagy and M.V. Diudea, in: *Nanostructures – Novel Architecture*, ed. M.V. Diudea (Nova, New York, 2004), in press.
[24] R.B. King, Discrete Math. 244 (2002) 203.
[25] A. Ceulemans, E. Lijnen, L.J. Ceulemans and P.W. Fowler, Mol. Phys. 102 (2004) 1149.
[26] M.V. Diudea, Stud. Univ. Babes-Bolyai, Chemia 48 (2003) 3.